Journal of Thermal Analysis and Calorimetry
https://doi.org/10.1007/s10973-024-13933-8

Reactivity of belite in calcium sulfoaluminate-based cements

Raquel Pérez-Bravo[1] · Imane Koufany[1] · Ana Cuesta[1] · Eric P. Bescher[2] · Miguel A. G. Aranda[1] · Isabel Santacruz[1] · Angeles G. De la Torre[1]

Received: 21 February 2024 / Accepted: 29 November 2024

Abstract
The hydration behavior of belite phase in different cements is not well understood. Belite hydrates very slowly but there are reports with faster hydration kinetics. Here, the hydration behavior of belite phase in a commercial belite calcium sulfoaluminate (BCSA) cement has been investigated. The BCSA cement was hydrated with two water-to-cement ratios, 0.50 and 0.65 and at two temperatures, 20 and 40 °C. Studies of calorimetry, NMR, laboratory X-ray powder diffraction (XRPD), thermal analysis (TA) of the pastes, and mass balance calculations have been performed. The calorimetric and LXRPD studies showed that with sufficient water for the hydration reactions to take place, i.e., $w/c = 0.65$, the degree of reaction of belite is 30% at 7 days and above 60% at 35 days, at 40 °C. The ^{29}Si and ^{27}Al MAS-NMR and TA studies confirmed the reactivity of belite under conditions of sufficient water (thermodynamic requirement) and at high temperature (kinetic requirement). This was demonstrated by the presence of stratlingite by ^{27}Al MAS-NMR and TA. Finally, it was found that ~ 12 mass% of the added water remains unbound, but it is unavailable for the progression of hydration reactions in the studied experimental conditions.

Keywords Belite reactivity · Water-to-cement ratio · Temperature · Calcium sulfoaluminate

Introduction

Cements containing calcium sulfoaluminate phase, also known as ye'elimite, are recognized as alternative low-carbon cements owing to their reduced lime content and lower manufacturing temperatures [1, 2]. There are two main families of ye'elimite-based cements: (i) those comprising over 60 mass% calcium sulfoaluminate, generally termed CSA, used to compensate shrinkage [3, 4], fast setting and for encapsulating radioactive wastes [5, 6] and (ii) those with high belite content, > 50 mass%, usually denoted as belite calcium sulfoaluminate (BCSA) or belite-ye'elimite-ferrite (BYF) [7, 8], for instance used for its rapid setting and high early mechanical strengths [9].

The hydration processes of these types of cements have undergone extensive investigations and strongly depend upon various parameters, including the type and quantity of calcium sulfate incorporated in the cement production [10–13], the water-to-cement ratio [14, 15], the temperature [16–18], the presence of reactive minor phases, or the use of retarders [19, 20]. All these studies agree that ye'elimite dissolves very quickly in water and, with an appropriate quantity of additional calcium sulfate, yields ettringite (also named as AFt) and amorphous hydrated aluminum hydroxide [21, 22] within minutes after water mixing, reaction (1). Hereafter, cement nomenclature will be employed.

$$C_4A_3\bar{S} + 2C\bar{S} + 48H \rightarrow C_6A\bar{S}_3H_{32} + 2(AH_3 \cdot 5H) \quad (1)$$

This reaction is the main responsible for the rapid setting and the early strength of CSA and BCSA.

Depending on the amount of sulfate [12], AFm can be formed by the reaction of ye'elimite with water according to reaction (2).

$$C_4A_3\bar{S} + 28H \rightarrow C_4A\bar{S}H_{12} + 2(AH_3 \cdot 5H) \quad (2)$$

These reactions are so fast that they can lead to poor workability, and consequently, the use of retarders is advisable [23, 24]. In addition, it has been published that ettringite

✉ Angeles G. De la Torre
mgd@uma.es

[1] Departamento de Química Inorgánica, Cristalografía y Mineralogía, Universidad de Málaga, 29071 Málaga, Spain

[2] 2021 Engineering V, Department of Materials Science and Engineering, University of California Los Angeles, Los Angeles, CA 90095, USA

Published online: 15 January 2025

transforms into AFm at higher temperatures as its solubility increases [25].

Belite is the major phase in BCSA and a minor phase, but in significant amounts, in CSA. However, its hydration behavior is not so well understood. It has been described to react, in this aluminum-rich environment, according to reaction (3) to form stratlingite [7], which is also an AFm-type phase.

$$C_2S + AH_3 \cdot 5H \rightarrow C_2ASH_8 \quad (3)$$

If the cement also contains iron in the form of ferrite, belite can react with it to form amorphous iron-siliceous hydrogarnet [26, 27].

At later ages, when all the AH_3·5H is consumed by reaction (3), belite further hydrates yielding amorphous C-S-H, according to reaction (4), assuming that the C-S-H gel has the same stoichiometry than that of alite [28].

$$C_2S + 4.3H \rightarrow 0.2CH + C_{1.8}SH_{4.0} \quad (4)$$

Although the presence of an amorphous C-S-H has been demonstrated in cements based on calcium sulfoaluminate [16, 18, 29], the degree of hydration of belite is very low at 28 days of hydration. In the last decade, several attempts have been performed aimed to increase the degree of hydration of belite by stabilizing highly reactive polymorphs of belite [30, 31] or by preparing alite-containing clinkers [32]. However, other authors highlighted its low reactivity coining the catchy term "*belite a waste of lime*" [33]. Consequently, the reactivity of belite and its role in the mechanical strengths required further studies and clarification.

In this work, the hydration of a commercially available BCSA cement is studied to understand the hydration behavior of belite, its major constituent. To do so, two water-to-cement ratios (thermodynamic approach) and two temperatures (kinetic approach) were tested. ^{27}Al and ^{29}Si MAS-NMR, calorimetry, thermal analysis and laboratory X-ray powder diffraction studies have been performed to unravel the effect of water availability and temperature on the kinetics of belite hydration.

Materials and methods

Materials

A BCSA cement was used. Table 1 shows the textural properties of this cement, i.e., particle size distribution measured by laser diffraction by applying MIE theory with non-spherical particles and with a refractive index (RI) of 1.68 and an absorption index (AI)of 0.1 [34], specific surface area (SSA) determined by the BET approximation of the N_2 isotherm and fineness determined by the air permeability method (Blaine). The elemental composition, expressed as oxides, the mineralogical composition and the textural properties are also reported in Table 1. A commercial citric acid (Sigma-Aldrich) was used as a retarder.

Paste preparation

The tested w/c ratios were 0.50 and 0.65. To ensure the workability of the pastes, a fixed amount of citric acid of 0.20 mass% by mass of cement (*bwc*) was used.

The pastes were prepared at 20 °C using a mechanical stirrer. They were then filled into cylindrical molds made of polytetrafluoroethylene, which were rotated in a roller

Table 1 Textural properties, elemental composition, expressed as weigh percentage of oxides, determined by XRF, including loss on ignition (LOI) and mineralogical composition determined by synchrotron X-ray powder diffraction (SXRPD) and Rietveld method

Textural properties			
$D_{v,10}$/μm	0.9	Density/g cm^{-3}	2.98
$D_{v,50}$/μm	8.6	SSA/m^2 g^{-1}	2.06
$D_{v,90}$/μm	39.2	Blaine fineness/cm^2 g^{-1}	5909
Chemical composition from XRF/mass%		Mineralogical composition from SXRPD/mass%	
CaO	50.1	β-C_2S	45.1
Al_2O_3	14.9	α'_H-C_2S	5.8
SiO_2	14.3	Ortho-$C_4A_3\,\overline{S}$	27.9
SO_3	14.1	C $\overline{S}$	8.4
MgO	1.8	C $\overline{S}$ $H_{0.5}$	3.3
Fe_2O_3	0.9	Minors	9.4
K_2O	0.6		
Minors	1.4		
LOI	1.9		

table at 16 rpm for the first 24 h, at the same temperature. The pastes were demolded after 24 h and stored in a closed plastic container with water in a chamber at 20 ± 1 °C to be stopped at the appropriated ages. The 40 °C pastes were mixed in the same way as those at 20 °C, except they were sealed with plastic to avoid direct contact with water before being submerged. The roller table, cylinder molds, and water used for the curing process were at 40 °C before use, and the entire procedure was carried out in the stove at 40 °C. The ages chosen to stop the hydration of all the pastes were 1 and 7 days and ~ 1 and ~ 2 months. This process was carried out with manual grinding and two washes with isopropanol and one with diethyl ether [35]. After completion of the process, the samples were stored in a desiccator and sealed with a plastic polymer.

The pastes are referred below as BCSA_*X*wc_*Y* °C, where *X* stands for 0.50 or 0.65 and *Y* for 20 or 40.

Synchrotron X-ray powder diffraction (SXRPD)

The anhydrous sample was measured at ALBA synchrotron (Barcelona, Spain) in the diffraction end station of the Materials Science and Powder Diffraction (MSPD) beamline. The sample was mixed with quartz, ~ 30 mass%, as an internal standard to determine the amount of amorphous and non-quantified crystalline content (ACn) [36]. However, the amount of ACn calculated was very low. Consequently, the amorphous content, if present, is below the limit of quantification, i.e., ~ 5 mass%, so it is considered here as 0.0 mass%. To analyze this pattern and to obtain the Rietveld quantitative phase analysis (RQPA), the Rietveld method was applied using the GSAS II software package [37] with the instrumental parameters determined in a previous publication [38].

Laboratory X-ray powder diffraction (LXRPD) and data analysis

Before obtaining the powder patterns, the arrested-hydration pastes were manually mixed in an agate mortar with an internal standard, ~ 20 mass% of quartz, to determine the ACn content [36]. The LXRPD patterns for these mixtures were recorded using a D8 ADVANCE (Bruker AXS), Mo-$K_{\alpha 1}$, $\lambda = 0.7093$ Å and a θ/θ geometry, at the Servicios Centrales de Apoyo a la Investigación (SCAI) of the University of Málaga (UMA). To analyze these patterns, the Rietveld method was applied using the GSAS I software [39] using a pseudo-Voigt peak shape function [40] with the asymmetry correction [41]. The refined parameters were background coefficients, zero-shift error, phase scaling factors, unit cells, peak shape parameters and coefficient of preferred orientation (if required). The structural descriptions, CIF files, of the crystalline anhydrous and hydrated phases used in this analysis are published elsewhere [42, 43].

Magic angle spinning nuclear magnetic resonance (MAS-NMR) study

The pastes for the ^{29}Si MAS-NMR and the ^{27}Al MAS-NMR studies were prepared as described in section "Paste preparation". The equipment used, which is located at the SCAI at UMA, is described below: Bruker AVIII HD 600NMR (field strength of 14.1 T). The conditions for the ^{29}Si MAS-NMR measurements were with ^{1}H decoupling by single pulse excitation with a pulse $\pi/2$ of 5 µs, 30 s relaxation delay and 10,800 scans, working at 119.8 MHz with a 2.5-mm triple-resonance DVT probe using zirconium oxide rotors at 15 kHz spin rate, and the referenced external solution was tetramethylsilane (TMS). The conditions for the ^{27}Al MAS-NMR measurements were single pulses $\pi/12$ of 1 µs, 5 s relaxation delay and 2000 scans, 156.4 MHz and rotors operated at 20 kHz and the referenced external solution was 1 M $Al(NO_3)_3$.

Thermal analysis (TA)

The TA traces were measured using an SDT-Q600 analyzer by placing the samples in open platinum crucibles under air flow. The heating profile for the anhydrous BCSA was from room temperature (RT) to 1000 °C at 10 °C min^{-1}.

The pastes for this study were prepared as described in section "Paste preparation". The arrested-hydration pastes were measured without adding internal standard. The heating profiles were from RT to 40 °C (at 10 °C min^{-1}), isothermal at 40 °C for 30 min and heating to 1000 °C (at 10 °C min^{-1}). The water that is not chemically bound is referred to here as unbound water (UW) and is calculated using Eqs. (5) and (B), with all values given in percent by mass:

$$BW = \frac{BW_{ATD} \times CEM}{100 - BW_{ATD}} \quad (5)$$

$$UW = NW - BW \quad (6)$$

CEM stands for the cement content, BW for the chemically bound water, BW_{ATD} for the mass loss measured from 40 to 550 °C from TA curves, and NW for the nominally added water.

Isothermal calorimetry

Pastes for the calorimetric studies were prepared as described in section "Paste preparation". Immediately after preparation, they were poured into glass ampoules and inserted into the eight-channel thermal activity monitor

(TAM) calorimeter. The preparation and loading of the glass ampoules into the calorimeter took less than 10 min for all samples. The ampoules with water as the reference [44] were placed in the calorimeter, and the temperature signal was stabilized prior to loading the samples, allowing data collection to begin immediately after sample insertion. Measurements were conducted over 7- and 14-day periods at 20 °C and 40 °C.

Results and discussion

Calorimetry study

The BCSA pastes were prepared with two different w/c ratios, 0.50 and 0.65, as described in the experimental section. The w/c ratio of 0.50 is commonly used for field applications of these types of cements [45, 46]. This ratio leads to a significant fraction of the cement as unreacted because the lack of water. The second ratio was not chosen arbitrarily. The theoretical w/c ratio for a complete reaction of ye'elimite and belite was calculated on the basis of reactions (1) to (4), being 0.68. Therefore, from a theoretical point of view (and without considering the additional role of water as reaction environment for species diffusion), a w/c ratio of 0.65 could be sufficient for nearly complete reaction. Moreover, in addition to the commonly employed 20 °C for placing our results in the BCSA hydration landscape, reaction at 40 °C was also investigated in order to accelerate the kinetics of the hydration without significantly altering the resulting hydrates.

Figure 1a and b shows the heat flow up to 6 h and the cumulative heat of all pastes up to 72 h, respectively. The pastes hydrated at 40 °C were also measured up to 14 days and so the corresponding cumulative heat curves are included in Fig. 1b as an inset. It is known that this type of cement reacts very quickly [47], and here, it is observed that the main heat flow signals occur before 2 h after mixing cement with water.

The curve of the paste with the w/c ratio of 0.50 (at 20 °C) shows an intense signal centered at 1 h, related to the dissolution of ye'elimite and anhydrite and the precipitation of AFt and amorphous aluminum hydroxide [15]. On the one hand, the increase in the w/c ratio (at 20 °C) caused a change in the hydration mechanism, as evidenced by a splitting of the main signal and an acceleration effect. This effect has been previously observed [22] and may be related to a faster dissolution of ye'elimite by increasing the w/c ratio due to larger concentration gradients and the higher solubility of AFt at this temperature [25]. As expected, a slight increase in total heat at 72 h was observed by increasing the w/c ratio at 20 °C, Fig. 1b [15] due to a higher degree of hydration of ye'elimite. During the first three days, increasing the w/c ratio does not seem to have any effect on the belite hydration since the slight increase in total heat at 24 h can be justified by the higher degree of reaction of ye'elimite.

On the other hand, the increase in temperature led to an acceleration of hydration in both pastes, which is almost identical regardless of the w/c, dashed curves in Fig. 1. This can be observed by i) the absence of an induction period, ii) a sharper slope of the main signal, iii) earlier times for the maxima and, iv) larger values of these

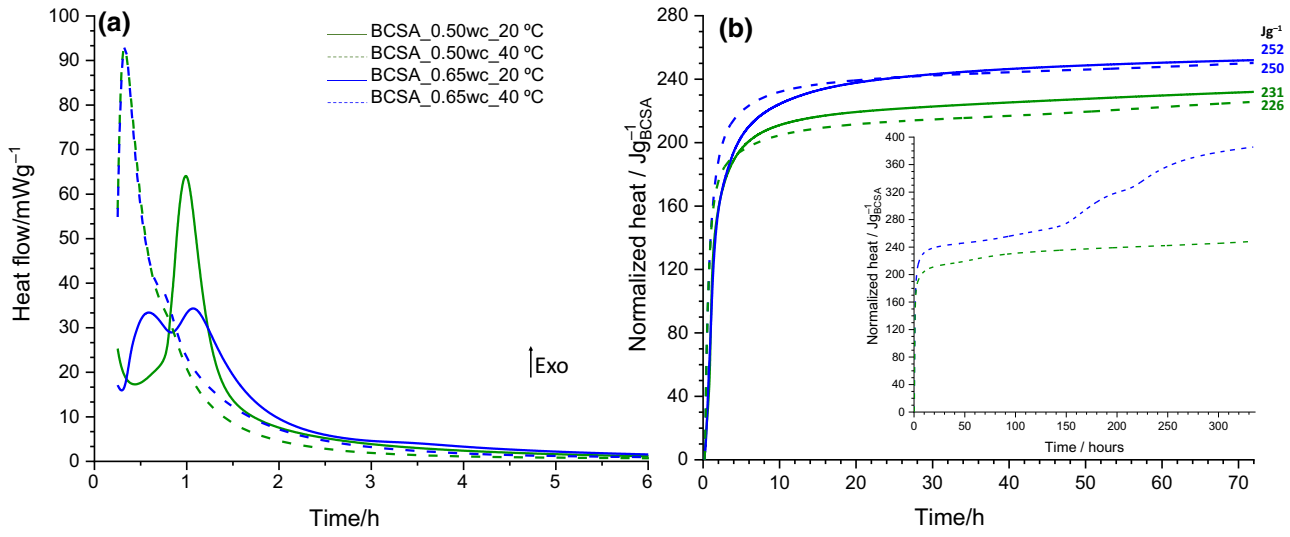

Fig. 1 Isothermal calorimetric curves of BCSA pastes, referenced to 1 g of binder, prepared with w/c ratios of 0.50 and 0.65, and at 20 °C and 40 °C. **a** Heat flow traces during the first 6 h, for better visualization. **b** Cumulative heat during the first three days of hydration. Inset in (**b**) shows two additional experiments carried out for the pastes with the two w/c ratios at 40 °C during 14 days. (Color figure online)

maxima. However, the heat released after 24 h is almost constant up to 72 h; consequently, it seems that belite reactivity is not enhanced at 40 °C. Therefore, the calorimetry of the pastes at 40 °C was extended to 14 days, see inset in Fig. 1. The cumulative heat of the sample with $w/c = 0.65$ shows an increase in heat that started at 6 days of hydration, while the trace for the sample with $w/c = 0.50$ remains stagnated. These data show that belite reactivity is kinetically enhanced (by temperature) only if there is sufficient amount of water for its double role: reactant and dissolution and transport medium.

^{29}Si and ^{27}Al MAS-NMR study

Figure 2 shows the ^{29}Si and ^{27}Al MAS-NMR spectra for the anhydrous and hydration-stopped pastes at selected hydration times. Three pastes were prepared for this section, BCSA_0.50wc_20 °C, BCSA_0.65wc_20 °C and BCSA_0.65wc_40 °C.

The ^{29}Si MAS-NMR spectra allow the local environment of the silicon atoms in each paste to be studied. All pastes show the resonance of unreacted C_2S, ~ -- 2 ppm, which is due to Q^0 species. In the paste BCSA_0.50wc_20 °C, the intensity of this signal is almost constant which shows that the reactivity of this phase is very low at a w/c of 0.50 and

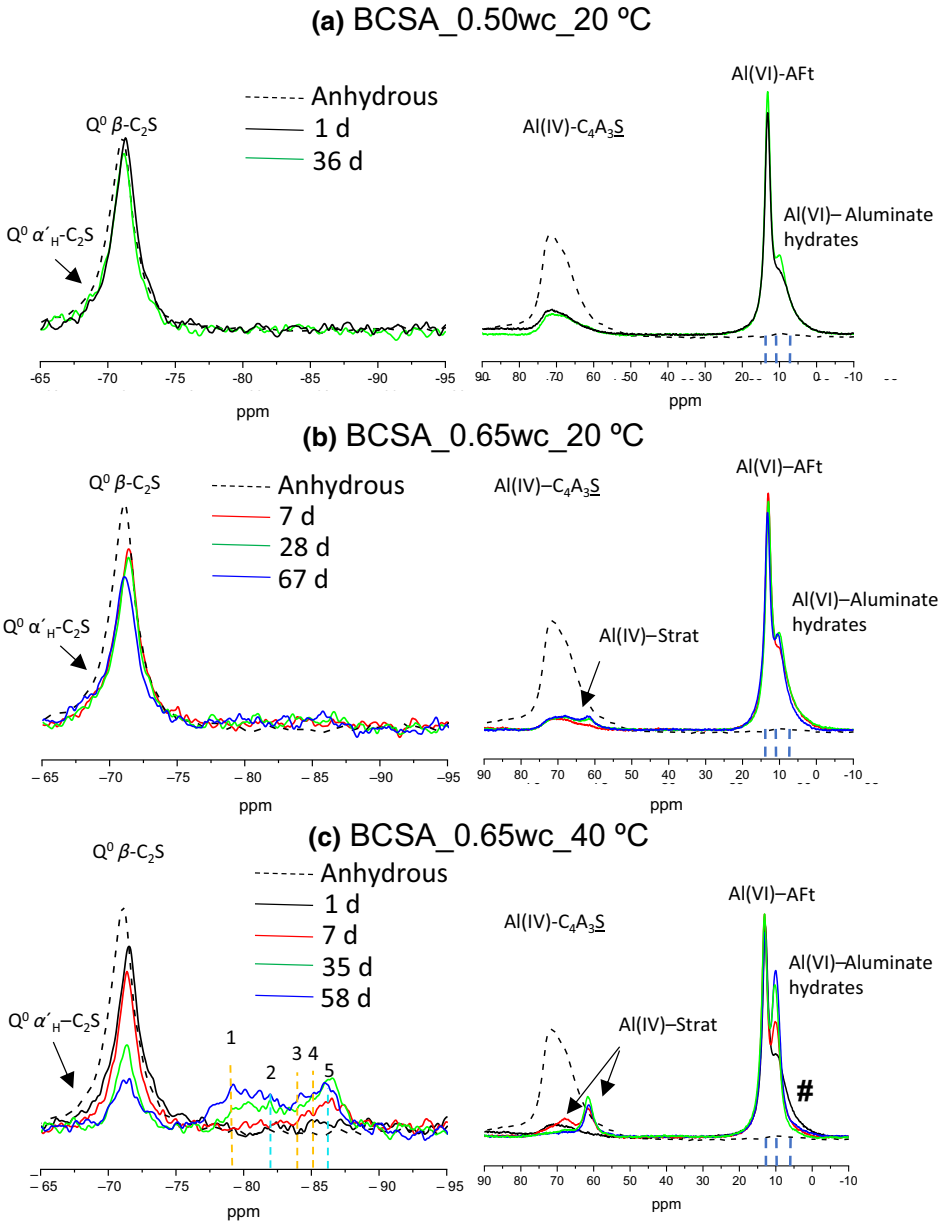

Fig. 2 ^{29}Si MAS-NMR (left panels) and ^{27}Al MAS-NMR (right panels) spectra of anhydrous BCSA and hydration-arrested pastes at selected hydration times. **1** stands for Q^1 of C-S-H gel; **2** and **5** stands for Q^2 of stratlingite; **3** stands for Q^2(1Al) of C-S-H gel; **4** stands for Q^2 of C-S-H gel. (Color figure online)

20 °C, even at 36 days of hydration. In contrast, a slight decrease in this signal is observed in $w/c = 0.65$ paste, indicating a slight increase in belite reactivity at 28 days, although there are no clear ^{29}Si resonances due to hydrated phases. These results indicate that the higher availability of water at 20 °C only slightly increases the reactivity of belite. The increase in temperature for the $w/c = 0.65$ paste confirms the calorimetry finding. At 7 days of hydration, the Q^2 signal due to stratlingite is already observed. Furthermore, at 35 and 58 days, there are also Q^n due to C-S-H gel [18, 29], see left panels in Fig. 2c.

The ^{27}Al MAS-NMR spectrum of anhydrous cement contains the signals related to the tetrahedral Al coordination, ~ 70 ppm, of ye'elimite. In all pastes, this signal decreases significantly indicating a high reactivity of ye'elimite, although it is not completely consumed in BCSA_0.50wc_20 °C and BCSA_0.65wc_20 °C even at 36 and 67 days, respectively (Fig. 2a and b, right panel). In addition, all spectra show the octahedral aluminum coordinate of ettringite, ~ 13 ppm, and aluminate hydrates, the latter with two signals, centered at ~ 10 ppm and ~ 5 ppm [48]. In the paste BCSA_0.50wc_20 °C, the main hydration products are AFt, which shows a sharp signal, and aluminum hydroxide gel with a broad band. Increasing the w/c ratio led to an increase in the intensity of the resonance centered at ~ 10 ppm and related to AFm-type phases [49], which in this case could be due to the formation of a minor amount of stratlingite at 7 days of hydration. Moreover, the Al(IV) signal of stratlingite is visible at ~ 62 ppm, indicating the increased reactivity of belite due to the higher water availability, Fig. 2b right panel, following reaction (3). The reactivity of belite in the BCSA_0.65wc_40 °C paste is clearly confirmed by two features in the ^{27}Al MAS-NMR spectra: i) the signals of stratlingite, ~ 68 and 62 ppm due to Al(IV) and ~ 10 ppm due to Al(VI), are much more intense, and ii) the decrease in the signal of aluminum hydroxide gel, ~ 5 ppm, with hydration time highlighted by a # in Fig. 2c, right panel.

Thermal analysis

Figure 3a and b shows the thermal curves of the hydration-arrested pastes BCSA_0.50wc_20 °C and BCSA_0.65wc_40 °C at selected hydration times, respectively. The amounts of unbound water were extracted from these data, and they are also discussed in the next section. In addition, qualitative information about the phase composition at each hydration age can also be obtained. All curves of BCSA_0.50wc_20 °C are almost identical from 7 to 61 days, confirming that the main reaction is the formation of AFt and aluminum hydroxide gel has already taken place at 1 day of hydration with only a minor contribution up to 7 days. Conversely, for BCSA_0.65wc_40 °C, the thermal curves change considerably with hydration time: i) signals due to the decomposition of AFm and stratlingite phases appear, and ii) the signal due to the dehydroxylation of aluminum hydroxide decreases from 1 to 7 days, indicating its consumption by stratlingite formation according to reaction (3).

Laboratory X-ray powder diffraction study

Figure 4a–c shows the LXRPD patterns of BCSA_0.50wc_20 °C, BCSA_0.65wc_20 °C and BCSA_0.65wc_40 °C at selected hydration times, respectively, with the peaks due to given phases labeled. Quartz was added after stopping the hydration as internal standard.

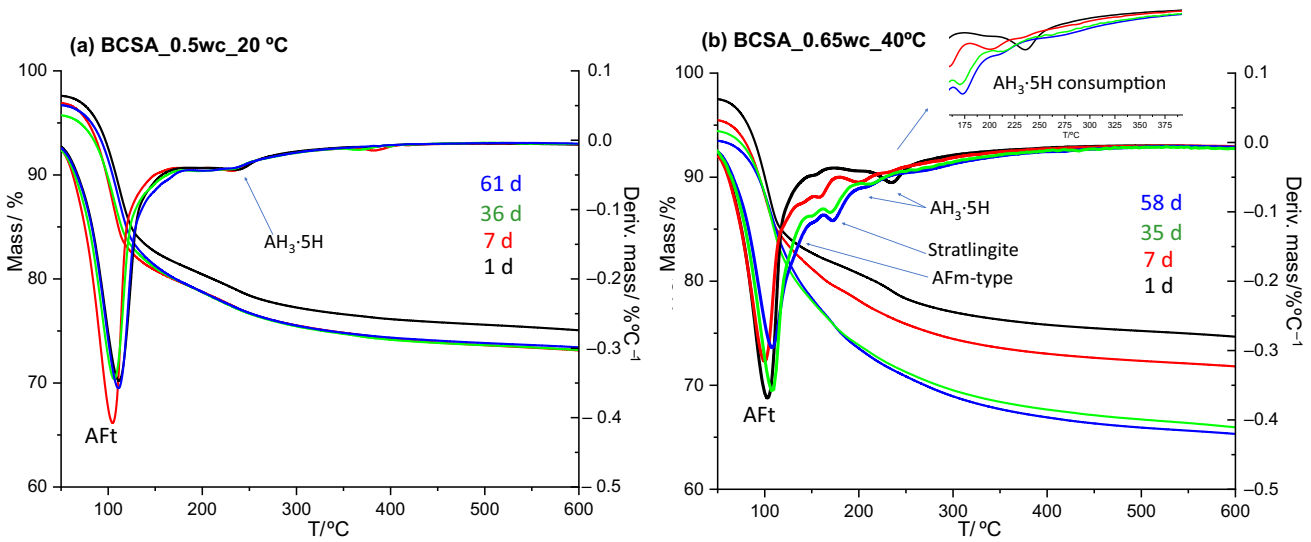

Fig. 3 Thermal analysis curves of **a** BCSA_0.50wc_20 °C and **b** BCSA_0.65wc_40 °C at selected hydration times. (Color figure online)

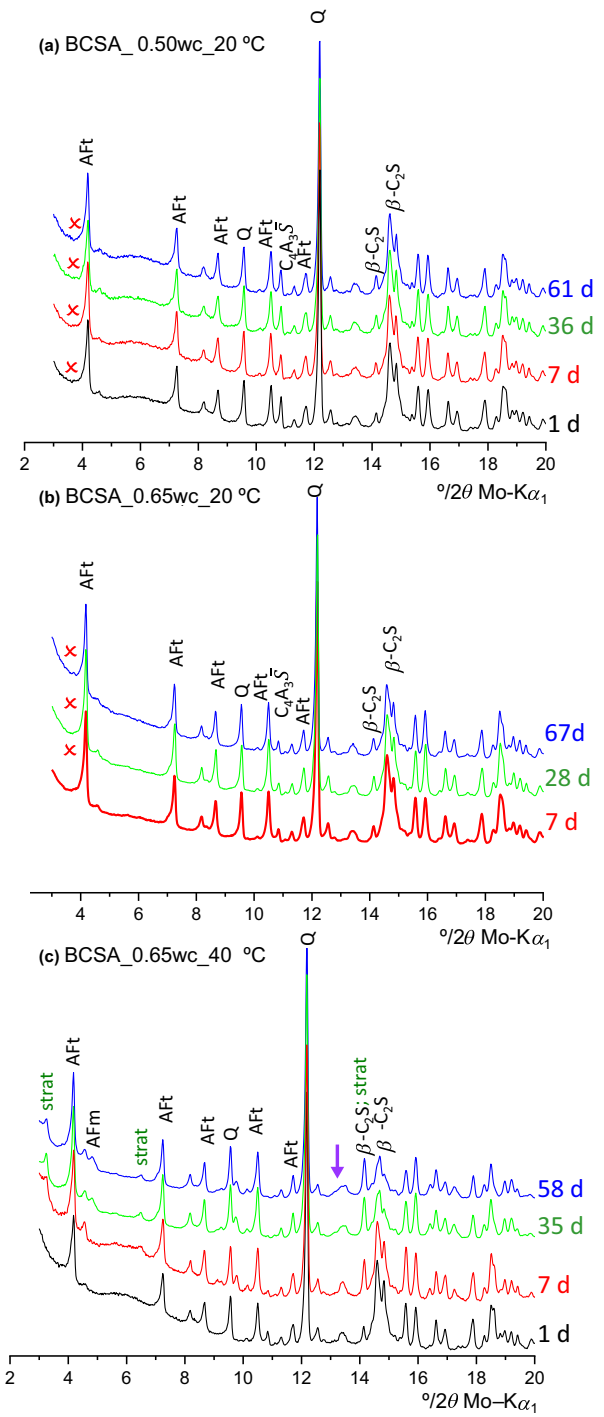

Fig. 4 LXRPD raw patterns for **a** BCSA_0.50wc_20 °C, **b** BCSA_0.65wc_20 °C and **c** BCSA_0.65wc_40 °C at selected hydration times with main peaks due to selected phases labeled. Red crosses in (**a**) and (**b**) highlight the absence of diffraction signals of crystalline stratlingite. Purple arrow in (**c**) highlights the C-S-H hump. (Color figure online)

All pastes show the diffraction signals of AFt regardless of w/c or temperature, which is due to the fast reaction of

Table 2 Phase assemblage of BCSA_0.50wc_20 °C at selected hydration ages, including ACn content determined by RQPA with the internal standard and unbound water (UW) by TA, referred to 100 g of paste

Phases\time	t_0	1	7	36	61
β-C_2S	30.1	28.1	28.5	27.6	26.4
α'_H-C_2S	3.9	0.8	0.7	0.5	0.4
ort-$C_4A_3\,\overline{S}$	18.6	3.6	3.0	3.2	3.0
$C\,\overline{S}$	5.6	1.3	1.3	1.2	1.1
$C\,\overline{S}\,H_{0.5}$	2.2	–	–	–	–
Minor	6.3	3.8	3.7	3.6	3.7
AFt	–	26.7	29.5	26.6	28.2
AFt_{calc}		*30.9*	*32.1*	*31.8*	*32.1*
Strat	–	–	–	–	–
$Strat_{calc}$		*12.5*	*11.7*	*14.1*	*17.6*
ACn	–	22.1	21.5	24.1	24.8
$AH_3{\cdot}5H_{calc}$		*4.9*	*5.7*	*4.2*	*2.3*
UW	**33.3**	**13.6**	**11.9**	**13.0**	**12.4**
UW_{calc}		*12.0*	*11.2*	*11.4*	*11.2*

Unbound water (UW), determined experimentaly from thermal data and equation (6), is shown in bold. In italics, results of mass balance calculations

ye'elimite with anhydrite. However, the diffraction peaks of stratlingite are only present in the pastes that have, not only a higher amount of water, but also a higher temperature, see Fig. 4c.

Tables 2–4 show the phase compositions of all pastes analyzed, referred to 100 g of paste. These results were obtained by combining two techniques, namely i) LXRPD and the Rietveld method on the arrested-hydration samples mixed with internal standard, which provides the mineralogical composition including the ACn content and ii) thermal analysis of the stopped hydration pastes, which allows the indirect determination of the unbound water (UW). These two approaches make it possible to obtain the complete phase composition of the pastes. These data permit the calculation of the degree of hydration, DoH, of ye'elimite and belite, and they are displayed in Fig. 5.

The reactivity of ye'elimite following reaction (1) is very fast and the DoH of this phase is above 80% already at one day of hydration for the $w/c = 0.50$ paste at 20 °C, increasing to 85% for $w/c = 0.65$ at the same temperature. The higher amount of water led to a slight increase in reactivity, but it was the increase in temperature that caused this phase to react to 100%. However, the molar ratio of ye'elimite to anhydrite in this cement is 1:1.8 (taking also bassanite into account), which is lower than that of reaction (1). Once anhydrite and bassanite are completely consumed at 40 °C, ye'elimite reacts further to give AFm according to reaction (2), as previously described in similar systems [17].

The effects of water amount and temperature on the DoH of belite follow a very similar trend to that described just

Table 3 Phase assemblage of BCSA_0.65wc_20 °C given as in Table 2

Phases\time	t_0	7	28	67
β-C_2S	27.4	26.2	23.8	23.1
α'_H-C_2S	3.5	0.5	0.4	0.4
ort-$C_4A_3\,\overline{S}$	16.8	1.3	1.2	1.4
C $\overline{S}$	5.1	1.0	0.9	1.0
C $\overline{S}$ $H_{0.5}$	2.0	–	–	–
Minor	5.6	3.1	3.2	3.9
AFt	–	28.5	31.7	31.7
AFt_{calc}		*32.1*	*32.3*	*31.9*
Strat	–	–	–	–
$Strat_{calc}$		*10.3*	*16.5*	*17.9*
ACn	–	19.6	20.6	22.1
$AH_3{\cdot}5H_{calc}$		*6.5*	*3.1*	*1.9*
UW	**39.4**	**19.7**	**18.2**	**16.3**
UW_{calc}		*17.3*	*17.2*	*17.4*

Unbound water (UW), determined experimentaly from thermal data and equation (6), is shown in bold. Italicized values represent the percentage of hydrated phases and unbound water, calculated using Eqs. (1) to (4) and the mass balance presented in Fig. 6

above for ye'elimite. On the one hand, increasing the w/c ratio at 20 °C slightly increases the DoH of total belite, Fig. 5, but despite the higher availability of water, the reaction kinetics of belite are very slow at 20 °C, with ~ 20% DoH, in agreement with [18]. Belite reacts according to reaction (3) consuming part of the hydrated aluminum hydroxide and forming stratlingite, which must be amorphous at 20 °C as no signals are detected in the LXRPD patterns, Fig. 4a and b. In addition, with the w/c ratio of 0.65 and 40 °C the DoH of belite increased significantly, over 60% at 35 days, resulting in a larger amount of crystalline stratlingite. In addition, a small hump, arrow in Fig. 4c, can be observed in the 58 days pattern, indicating the formation of a C-S-H gel from the hydration of belite according reaction (4). This behavior differs greatly from that recently reported [18], which shows that the reactivity of belite does not increase with temperature at 28 days of hydration. This could be due to the fact that the clinkers used in the two studies differ in the manufacturing process. The clinker used in this study is a commercial one produced with natural raw materials and has a slightly higher sulfur content (~ 7.3 mass% SO_3 versus 6.3 mass% [18]; considering that anhydrite was added to produce the cement). The presence of sulfur and other doping elements in the crystal structure of belite may have led to a distortion [50, 51] that makes it more reactive.

Table 4 Phase assemblage of BCSA_0.65wc_40 °C given as in Table 2

Phases\time	t_0	1	7	35	58
β-C_2S	27.4	26.9	21.6	11.4	8.6
α'_H-C_2S	3.5	0.5	–	–	–
ort-$C_4A_3\,\overline{S}$	16.8	1.5	0.6	–	–
C $\overline{S}$	5.1	1.0	–	–	–
C $\overline{S}$ $H_{0.5}$	2.0	–	–	–	–
Minor	5.6	3.9	4.2	3.4	3.2
AFt	–	24.3	27.6	28.9	26.5
AFt_{calc}		*31.6*	*31.6*	*31.6*	*31.6*
Strat	–	–	6.9	9.8	7.5
$Strat_{calc}$		*8.6*	*22.8*	*22.8*	*22.8*
AFm	–	–	3.6	6.2	7.1
AFm_{calc}		–	*0.9*	*1.5*	*1.5*
ACn	–	21.3	15.9	29.0	33.5
$AH_3{\cdot}5H_{calc}$		7.3	0.0	0.0	0.0
C-S-H_{calc}		–	–	13.7	17.6
CH_{calc}				0.9	1.1
UW	**39.4**	**21.1**	**19.7**	**11.4**	**13.6**
UW_{calc}		*17.6*	*16.9*	*11.8*	*10.5*

Unbound water (UW), determined experimentaly from thermal data and equation (6), is shown in bold. Italicized values represent the percentage of hydrated phases and unbound water, calculated using Eqs. (1) to (4) and the mass balance presented in Fig. 6

At this point, it is worth analyzing the results for UW obtained for the three pastes by TA, (Tables 2–4). The UW of the paste with w/c ratio of 0.5 at 20 °C is 13.6 mass% and almost stagnates up to 61 days of hydration. Although this amount of water could be considered sufficient to continue the reactions, under these experimental conditions, this UW does not seem to be available as the reactions do not progress. This fact was also confirmed by calorimetry, as the heat evolved by the paste with w/c ratio of 0.50 and at 40 °C stagnates at ~ 230 Jg^{-1} at 14 days of hydration, inset in Fig. 1b, indicating that at higher temperatures the unbound water is not available to drive the reactions forward. Interestingly, the cement paste with higher w/c ratio, i.e., 0.65, shows a different behavior at 20 °C. The UW decreases continuously until 67 days of hydration, reaching a value of 16.3 mass%. The degree of ye'elimite reaction is slightly higher at all ages, Fig. 5, which is due to the higher water availability. However, despite the availability of water, no significant increase in the degree of reaction of belite is observed, demonstrating the slow hydration kinetics of this phase at this temperature. For the paste with the same amount of water but at a higher temperature, i.e., 40 °C, it is observed that belite has greatly increased its DoH and forms larger amounts of stratlingite according to reaction (3). Ye'elimite reaches a reaction degree of 100% in this paste, and the belite continues to react from 35 to 58 days. The unbound water stagnates after 35 days.

These experimental results are compared to the calculated amounts of hydration products and consumed water, which are obtained through detailed mass balance calculations outlined just below.

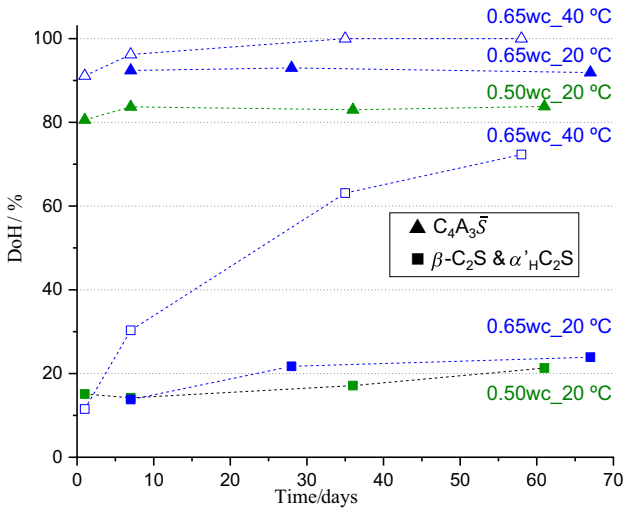

Fig. 5 Degree of hydration of ye'elimite (triangles) and total belite, i.e., β-C_2S and α'_H-C_2S (squares) at *w/c* 0.50 (green) and 0.65 (blue) and 20 °C (solid symbols) and 40 °C (open symbols). (Color figure online)

Mass balance calculations

The calculated hydrated products (crystalline and amorphous) and the calculated consumption of water were obtained using the phase composition results given in Tables 2–4, using reactions (1)–(4) and the mass balance calculations illustrated in Fig. 6. The calculation procedure is described next.

Step 1 The reacted ye'elimite is used to calculate the amount of AFt and the amorphous hydrated aluminum hydroxide according to reaction (1).

Step 2 When crystalline AFm is quantified, the reacted ye'elimite (considering the previous age when no AFm was present) is calculated according to reaction (2) to obtain calculated AFm and amorphous hydrated aluminum hydroxide.

Step 3 The reacted C_2S is computed in reaction (3) by consuming the calculated amorphous hydrated aluminum hydroxide and yielding stratlingite. If the calculated aluminum hydroxide is not completely consumed, the mass balance calculations end here.

Step 4 If the calculated aluminum hydroxide from steps 1 and 2 is consumed in step 3, and reacted C_2S still remains, this is computed with reaction (4), whereby amorphous C-S-H gel and Portlandite are formed.

The total BW is also calculated by steps 1, 2 and 4.

Tables 2–4 contain the results of the mass balance calculations. It should be noted the three following considerations in the employed approach.

(i) The AFt_{calc} content from reaction (1) is calculated considering ye'elimite as limiting reactant;

(ii) The amorphous fraction content depends on the reactivity of the paste. If AFt or AFm are the only crystalline phases, the amorphous fraction is composed of the remaining $AH_3{\cdot}5H_{calc}$ not consumed by reaction (3) and the calculated stratlingite, i.e., $AH_3{\cdot}5H_{calc} + strat_{calc}$ (Tables 2 and 3). If crystalline stratlingite is also observed, the amorphous fraction is $AH_3{\cdot}5H_{calc} + strat_{calc} - strat_{exp} + C\text{-}S\text{-}H_{calc} + CH_{calc}$ (Table 4).

(iii) The amount of water consumed, BW, is computed by reactions (1), (2) and (4).

The results for AFt are discussed first. Figure 7a shows the experimentally measured and calculated amounts of crystalline AFt for BCSA_0.50wc_20 °C. In this case, the AFt calculated from the reactivity of ye'elimite is on average 4 mass% higher than the AFt

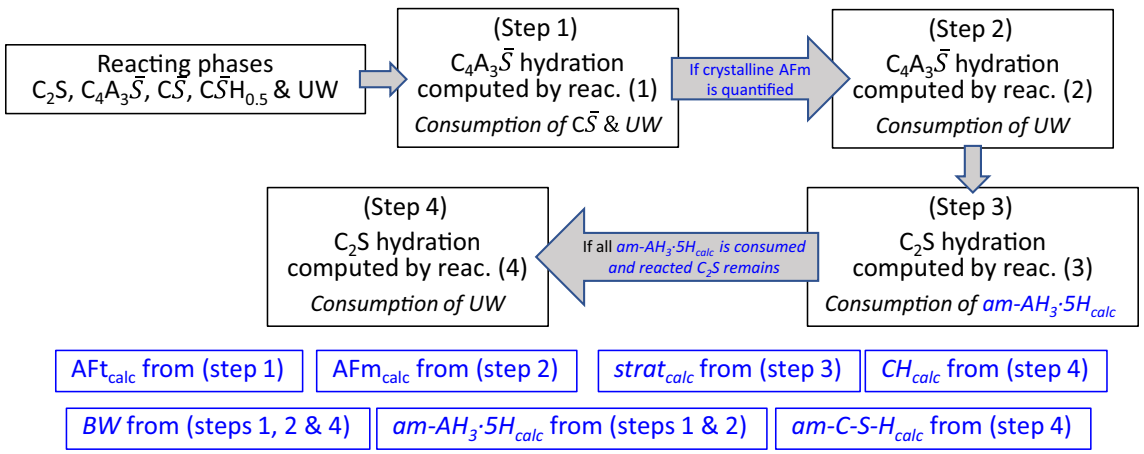

Fig. 6 Graphical illustration of mass balance calculations

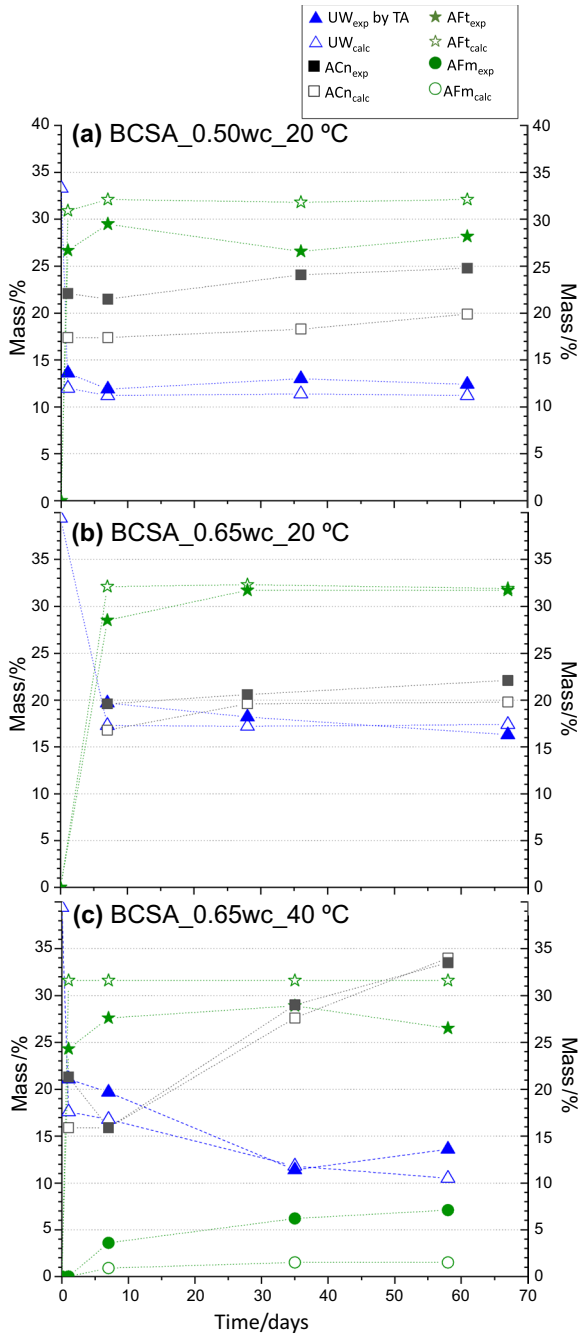

Fig. 7 Calculated (open symbols) and experimental amounts of UW (triangles), ACn (squares), AFt (stars) and AFm (circles) for **a** BCSA_0.50wc_20 °C, **b** BCSA_0.65wc_20 °C and **c** BCSA_0.65wc_40 °C

determined experimentally by RQPA and normalized with the UW obtained by TA (Fig. 7a). However, in the paste BCSA_0.65wc_20 °C, Fig. 7b, this discrepancy is not observed, and the values are in good agreement. This can be interpreted by assuming a small amount of amorphous ettringite present in the w/c = 0.50 paste. For BCSA_0.65wc_40 °C, Fig. 7c, the difference is similar to the BCSA_0.50wc_20 °C paste, where the experimental AFt is 4–5 mass% lower than the calculated value. For this sample, the difference could be due to the presence of crystalline AFm, which causes major uncertainties in the mass balance calculations. For AFm phases, it is known that the interlayer species can largely vary [52]. This highlights some limitations in the mass balance calculations where assumptions and simplifications must be done.

The comparison between the calculated and the experimental ACn is also shown in Fig. 7. The agreement is good, despite the limitations of the methodology mentioned in the previous paragraph.

Finally, the UW contents are discussed. The trend determined by TA and mass balance calculation is consistent for all pastes, and the absolute values are in good agreement. The experimental and calculated UW values in the pastes with a water/cement ratio of 0.50 at 20 °C and that with 0.65 at 40 °C stagnate at ~ 12 mass%. To interpret these results, the types of water in cement hydration should be considered. Water has a twofold role: Water as a medium for dissolution and mass transport and as a reactant. Firstly, water is the medium, in which solid phases (crystalline and amorphous) are dissolved. After mass transport, when oversaturation is reached, a certain hydrated phase precipitates, with water playing the second role as a reactant. In the mass balance calculations, water is only considered as a reactant. In addition, there is a fraction of the water that is physically adsorbed onto the surfaces of the particles and also filling the pores of the amorphous components. This water is neither available as a reactant nor as a medium and cannot be estimated by mass balance calculations. The available water fills large capillary pores acting as a medium and as a reactant [53, 54]. Therefore, ~ 12 mass% of UW (on the basis of 100 g of paste) appears to be the quantity of adsorbed/interacting water that is unavailable to facilitate the progression of hydration reactions.

Conclusions

For the studied BCSA cement, the calorimetric study revealed that pastes with a w/c ratio of 0.50 at both 20 °C and 40 °C showed stagnant heat release after 24 h, indicating insufficient water to sustain hydration. In contrast, pastes with a w/c ratio of 0.65 at 40 °C continued releasing heat after 6 days, highlighting accelerated belite hydration when more water is available.

LXRPD studies confirmed these findings, showing that increasing the w/c ratio at 20 °C slightly increased the degree of hydration (DoH) of belite (~ 20% from 28 to 67 days). For pastes with a w/c ratio of 0.50 at 20 °C, the unbound water remained constant (~ 13%) from 1 to 61 days, indicating that this water was unavailable for further reactions. Increasing

the w/c ratio to 0.65 led to a gradual decrease in unbound water (~ 16% at 67 days), but no significant increase in belite hydration was observed at 20 °C due to its slow kinetics at this temperature.

At 40 °C and $w/c = 0.65$, significant belite hydration occurred, with DoH exceeding 60% by 35 days, alongside the formation of stratlingite. Here, the unbound water stagnated at ~ 12%, suggesting that this amount represents physically adsorbed water, which does not facilitate further hydration.

NMR and thermal analyses corroborated these results, confirming stratlingite formation and amorphous hydrated aluminum hydroxide consumption under these conditions.

In summary, belite hydration requires more than 12% unbound water, but at 20 °C, the reaction remains slow even with sufficient water. At 40 °C, hydration is accelerated, reaching 60% DoH at 35 days when water is available, but the reaction halts once unbound water reaches ~ 12%.

Acknowledgements PID2020-114650RB-I00, which are cofunded by ERDF, from the Spanish government is gratefully acknowledged. CSA Research LLC is thanked for the donation to fund young scientists. Dr. Daniel Camas from Dpt. Ingeniería Civil, de Materiales y Fabricación of UMA is thanked for allowing the use of their mechanical strength device. ALBA synchrotron is acknowledged for providing with beamtime at MSPD beamline. Funding for open access charge: Universidad de Málaga/CBUA.

Author contributions This work is part of R Pérez-Bravo PhD work and involved in investigation, methodology, review and editing; I. Koufany involved in investigation, methodology, and review and editing; A. Cuesta involved in investigation, methodology, and review and editing; EP Bescher involved in review and editing; MAG Aranda involved in conceptualization, investigation, and review and editing; I Santacruz involved in investigation, funding acquisition, supervision, and review and editing; AG De la Torre involved in conceptualization, funding acquisition, supervision, writing original draft, and review and editing.

Funding Funding for open access publishing: Universidad Málaga/CBUA.

Data availability The raw data are freely deposited on Zenodo at https://doi.org/10.5281/zenodo.10604538. Data availability: SXRPD pattern of anhydrous cement (1 file), LXRPD of pastes (11 files), isothermal calorimetry raw data (4 files), TA curves (8 files) and ^{29}Si MAS-NMR and ^{27}Al MAS-NMR spectra (7 files).

References

1. Hanein T, De la Torre AG, Zhang Z, Provis JL. Alternative non-Portland binders in cement and concrete: from the Romans to Mars. Elem 18. 2022.
2. Gartner E, Hirao H. A review of alternative approaches to the reduction of CO_2 emissions associated with the manufacture of the binder phase in concrete. Cem Concr Res. 2015;78:126–42.
3. Chaunsali P, Mondal P. Influence of calcium sulfoaluminate (CSA) cement content on expansion and hydration behavior of various ordinary portland cement-CSA blends. J Am Ceram Soc. 2015;98:2617–24.
4. Péra J, Ambroise J. New applications of calcium sulfoaluminate cement. Cem Concr Res. 2004;34:671–6.
5. Nelson S, Geddes DA, Kearney SA, Cockburn S, Hayes M, Angus MJ, et al. Hydrate assemblage stability of calcium sulfoaluminate-belite cements with varying sulfate content. Constr Build Mater. 2023;383:131358.
6. Zhou Q, Milestone NB, Hayes M. An alternative to Portland cement for waste encapsulation—the calcium sulfoaluminate cement system. J Hazard Mater. 2006;136:120–9.
7. Aranda MAG, De la Torre AG. Sulfoaluminate cement. In: Pachelo-Torgal F, Jalali S, Labrincha J, editors. Eco-efficient concrete. Sawston: Woodhead Publishing; 2013. p. 488–522.
8. Gartner E, Sui T. Alternative cement clinkers. Cem Concr Res. 2017
9. Bescher E, Vallens K, Kim J. Belitic calcium sulfoaluminate cement: history, chemistry, performance, and use in the United States. In: Proceedings of the 1st international conference on innovation in low-carbon cement and concrete technology. Prague, Ch; 2019.
10. Chen IA, Hargis CW, Juenger MCG. Understanding expansion in calcium sulfoaluminate-belite cements. Cem Concr Res. 2012;42:51–60.
11. Paul G, Boccaleri E, Marchese L, Buzzi L, Canonico F, Gastaldi D. Low temperature sulfoaluminate clinkers: the role of sulfates and silicates on the different hydration behavior. Constr Build Mater. 2021;268:121111.
12. Rolland L, Trauchessec R, Institut DL, Lamour J, Le RB. Impact of anhydrite proportion in a calcium sulfoaluminate cement and Portland cement blend. Adv Cem Res. 2014;26:325–33.
13. Shen Y, Li X, Chen X, Zhang W, Yang D. Synthesis and calorimetric study of hydration behavior of sulfate-rich belite sulfoaluminate cements with different phase compositions. J Therm Anal Calorim. 2018;133:1281–9.
14. Pérez-Bravo R, Morales-Cantero A, Bruscolini M, Aranda MAG, Santacruz I, De la Torre AG. Effect of boron and water-to-cement ratio on the performances of laboratory prepared Belite-Ye'elimite-Ferrite (BYF) cements. Materials (Basel). 2021;14:4862.
15. Burris LE, Kurtis KE. Water-to-cement ratio of calcium sulfoaluminate belite cements: hydration, setting time, and strength development. Cement. 2022;8:100032.
16. Borštnar M, Daneu N, Dolenec S. Phase development and hydration kinetics of belite-calcium sulfoaluminate cements at different curing temperatures. Ceram Int. 2020;46:29421–8.
17. Xu L, Tang C, Li H, Wu K, Zhang Y, Yang Z. Hydration characteristics assessment of a binary calcium sulfoaluminate-anhydrite cement related with environment temperature. J Therm Anal Calorim. 2022;147:3053–61.
18. Chitvoranund N, Lothenbach B, Londono-Zuluaga D, Winnefeld F, Scrivener K. Influence of temperature on phase assemblages of belite-ye'elimite cement. Cem Concr Res. 2023;174:107339.

19. Bullerjahn F, Zajac M, Ben Haha M, Scrivener KL. Factors influencing the hydration kinetics of ye'elimite; effect of mayenite. Cem Concr Res. 2019;116:113–9.
20. Bullerjahn F, Zajac M, Skocek J, Ben HM. The role of boron during the early hydration of belite ye'elimite ferrite cements. Constr Build Mater. 2019;215:252–63.
21. Cuesta A, De la Torre AG, Santacruz I, Trtik P, Da Silva JC, Diaz A, et al. Chemistry and mass density of aluminum hydroxide gel in eco-cements by ptychographic X-ray computed tomography. J Phys Chem C. 2017;121:3044–54.
22. Bullerjahn F, Boehm-Courjault E, Zajac M, Ben Haha M, Scrivener KL. Hydration reactions and stages of clinker composed mainly of stoichiometric ye'elimite. Cem Concr Res. 2019;116:120–33.
23. Burris LE, Kurtis KE. Influence of set retarding admixtures on calcium sulfoaluminate cement hydration and property development. Cem Concr Res. 2018;104:105–13.
24. Zajac M, Skocek J, Bullerjahn F, Ben HM. Effect of retarders on the early hydration of calcium-sulpho-aluminate (CSA) type cements. Cem Concr Res. 2016;84:62–75.
25. Perkins RB, Palmer CD. Solubility of ettringite (Ca6[Al(OH)6]2(SO4)3 · 26H2O) at 5–75°C. Geochim Cosmochim Acta. 1999;63:1969–80.
26. Cuesta A, De la Torre AG, Santacruz I, Diaz A, Trtik P, Holler M, et al. Quantitative disentanglement of nanocrystalline phases in cement pastes by synchrotron ptychographic X-ray tomography. IUCrJ. 2019;6:473–91.
27. Dilnesa BZ, Wieland E, Lothenbach B, Dähn R, Scrivener KL. Fe-containing phases in hydrated cements. Cem Concr Res. 2014;58:45–55.
28. Cuesta A, Zea-Garcia JD, Londono-Zuluaga D, De la Torre AG, Santacruz I, Vallcorba O, et al. Multiscale understanding of tricalcium silicate hydration reactions. Sci Rep. 2018;8:8544.
29. Zea-Garcia JD, De la Torre AG, Aranda MAG, Santacruz I. Processing and characterisation of standard and doped alite-belite-ye'elimite ecocement pastes and mortars. Cem Concr Res. 2020;127:105911.
30. Alvarez-Pinazo G, Santacruz I, León-Reina L, Aranda MAG, De La Torre AG. Hydration reactions and mechanical strength developments of iron-rich sulfobelite eco-cements. Ind Eng Chem Res. 2013;52:16606–14.
31. Li GS, Gartner EM. High-belite sulfoaluminate clinker: fabrication process and binder preparation. World Patent Appl WO. 2006;18569:A2.
32. Hu Y, Li W, Ma S, Wang Q, Zou H, Shen X. The composition and performance of alite-ye'elimite clinker produced at 1300 °C. Cem Concr Res. 2018;107:41–8.
33. Scrivener KL, Matschei T, Georget F, Juilland P, Mohamed AK. Advances in hydration and thermodynamics of cementitious systems. Cem Concr Res. 2023;174:107332.
34. Merkus HG. Laser diffraction. Part Size Meas. 2009;259–85.
35. Snellings R, Chwast J, Cizer Ö, De Belie N, Dhandapani Y, Durdzinski P, et al. Report of TC 238-SCM: hydration stoppage methods for phase assemblage studies of blended cements—results of a round robin test. Mater Struct Constr. 2018;51:1–12.
36. De la Torre AG, Bruque S, Aranda MAG. Rietveld quantitative amorphous content analysis. J Appl Crystallogr. 2001;34:196–202.
37. Toby BH, Von Dreele RB, IUCr. GSAS-II: the genesis of a modern open-source all purpose crystallography software package. urn:issn:0021–8898. 2013;46:544–9.
38. Morales-Cantero A, Cuesta A, De la Torre AG, Santacruz I, Mazanec O, Borralleras P, et al. C-S-H seeding activation of Portland and belite cements: an enlightening in situ synchrotron powder diffraction study. Cem Concr Res. 2022;161:106946.
39. Larson AC, Von Dreele RB. General structure analysis system (GSAS). Los Alamos Natl Lab Rep LAUR. 2004;748:86–748.
40. Thompson P, Cox DE, Hastings JB. Rietveld refinement of debye-scherrer synchrotron X-ray data from A1203. J Appl Crystallogr. 1987;20:79–83.
41. Finger LW, Cox DE, Jephcoat AP. Correction for powder diffraction peak asymmetry due to axial divergence. J Appl Crystallogr. 1994;27:892–900.
42. De la Torre AG, Santacruz I, Cuesta A, León-Reina L, Aranda MAG. Diffraction and crystallography applied to anhydrous cements. In: Pöllmann H, editor. Cementitious materials: composition, properties, application. De Gruyter; 2017. p. 3–29.
43. Aranda MAG, Cuesta A, De la Torre AG, Santacruz I, León-Reina L. Diffraction and crystallography applied to hydrating cements. In: Pöllmann H, editor. Cementitious materials: composition, properties, application. Berlin: De Gruyter; 2017. p. 31–60.
44. Wadsö I. Isothermal microcalorimetry near ambient temperature: an overview and discussion. Thermochim Acta. 1997;294:1–11.
45. Ben Haha M, Winnefeld F, Pisch A. Advances in understanding ye'elimite-rich cements. Cem Concr Res. 2019;123:105778.
46. Koga GY, Albert B, Nogueira RP. On the hydration of Belite-Ye'elimite-Ferrite (BYF) cement pastes: effect of the water-to-cement ratio and presence of fly ash. Cem Concr Res. 2020;137:106215.
47. Winnefeld F, Barlag S. Calorimetric and thermogravimetric study on the influence of calcium sulfate on the hydration of ye'elimite. J Therm Anal Calorim. 2010;101:949–57.
48. Paul G, Boccaleri E, Cassino C, Gastaldi D, Buzzi L, Canonico F, et al. Fingerprinting the hydration products of hydraulic binders using snapshots from time-resolved in situ multinuclear MAS NMR spectroscopy. J Phys Chem C. 2021;125:9261–72.
49. Jones MR, Macphee DE, Chudek JA, Hunter G, Lannegrand R, Talero R, et al. Studies using 27Al MAS NMR of AFm and AFt phases and the formation of Friedel's salt. Cem Concr Res. 2003;33:177–82.
50. Morsli K, De la Torre AG, Zahir M, Aranda MAG. Mineralogical phase analysis of alkali and sulfate bearing belite rich laboratory clinkers. Cem Concr Res. 2007;37:639–46.
51. Yamashita M, Tanaka H, Sakai E, Tsuchiya K. Mineralogical study of high SO_3 clinker produced using waste gypsum board in a cement kiln. Constr Build Mater. 2019;217:507–17.
52. Matschei T, Lothenbach B, Glasser FP. The AFm phase in Portland cement. Cem Concr Res. 2007;37:118–30.
53. Flatt RJ, Scherer GW, Bullard JW. Why alite stops hydrating below 80% relative humidity. Cem Concr Res. 2011;41:987–92.
54. Lura P, Winnefeld F, Fang X. A simple method for determining the total amount of physically and chemically bound water of different cements. J Therm Anal Calorim. 2017;130:653–60.